https://doi.org/10.5194/gmd-2021-279
Preprint. Discussion started: 11 November 2021

Geoscientific Model Development Discussions

ECOSMO II(CHL): a marine biogeochemical model for the North Atlantic and the Arctic

Veli Çağlar Yumruktepe[1], Annette Samuelsen[1], Ute Daewel[2]

[1] Nansen Environmental and Remote Sensing Center, Jahnebakken 3, N-5007, Bergen, Norway
[2] Helmholtz-Zentrum Hereon, Institute for Coastal Systems – Analysis and Modelling, Max-Planck-Str. 1, Geesthacht, Germany

Correspondence to: Veli Çağlar Yumruktepe (caglar.yumruktepe@nersc.no)

Abstract. ECOSMO II is a fully coupled bio-physical model of 3d-hydrodynamics with an intermediate complexity N(utrient) P(hytoplankton) Z(ooplankton) D(etritus) type biology including sediment-water column exchange processes originally formulated for the North Sea and Baltic Sea. Here we present an updated version of the model incorporating chlorophyll a as a prognostic state variable: ECOSMO II(CHL). The version presented here is online coupled to the HYCOM ocean model. The model is intended to be used for regional configurations for the North Atlantic and the Arctic incorporating coarse to high spatial resolutions for hind-casting and operational purposes. We provide the full descriptions of the changes in ECOSMO II(CHL) from ECOSMO II and provide the evaluation for the inorganic nutrients and chlorophyll variables, present the modeled biogeochemistry of the Nordic Seas and the Artic and experiments on various parameterization sets as use cases targeting chlorophyll a dynamics. The model evaluations demonstrated that the simulations are consistent with the large-scale climatological nutrient settings, and are capable of representing regional and seasonal changes. The Norwegian and Barents Seas primary production show distinct seasonal patterns with a pronounced spring bloom dominated by diatoms and low biomass during winter months. The Norwegian Sea annual primary production is around double that of the Barents Sea while also having an earlier spring bloom. The parameterization experiments showed that the representation of open ocean chlorophyll a benefits from using higher phytoplankton growth and zooplankton grazing rates with less photosynthesis efficiency compared to the original implementation of ECOSMO II, which was valid for the North Sea and the Baltic Sea representing coastal domains. Thus, for open ocean modeling studies, we suggest the use of the parameterization sets presented in this study.

1 Introduction

Operational ocean forecasting and reanalysis systems that integrate in situ measurements, remote sensing observations, modelling and data-assimilation are fundamental tools for understanding the variability and dynamics of the physical and biogeochemical ocean state. Such systems are also essential for a better and more sustainable management of the oceans and marine ecosystems, supporting the development and understanding of human activities and the blue economy (von

https://doi.org/10.5194/gmd-2021-279
Preprint. Discussion started: 11 November 2021


Geoscientific Model Development Discussions

Schuckmann et al., 2016). In this context, the presentation of the underlying science, continuous evaluation and development of the forecast systems are required to provide the best possible forecast and reanalysis.

The presented model version, ECOSMO II(CHL), is adapted from the biogeochemical model ECOSMO (Schrum et al., 2006; S2006), later ECOSMO II (Daewel and Schrum, 2013; DS2013), and is currently used as the marine biogeochemical model for operational forecasts of the Arctic Ocean (ARC MFC – Arctic Marine Forecasting Centre) under the umbrella of CMEMS (The European Copernicus Marine Environment Monitoring Service; marine.copernicus.eu). The biogeochemical forecast ECOSMO II(CHL) has been operational since April 2017 and the daily values of selected variables can be retrieved from the CMEMS database. While based on the ECOSMO II version presented in DS2013, the transfer of the model to a different circulation model, region, and model resolution necessitated an adjustment of model parameterizations and additional functionalities, which in turn required a series of new sensitivity tests.

ECOSMO II is an intermediate complexity nutrient-phytoplankton-zooplankton-detritus (NPZD) type model describing the trophic interactions between three phytoplankton and two zooplankton components. It was shown to successfully simulate the seasonal and inter-annual ecosystem variability of primary and secondary production in the North- and Baltic Sea (Daewel and Schrum, 2013). In the framework of the ARC MFC forecasting system which covers the northern part of the Atlantic Ocean and the Arctic, its application and scientific scope was shifted to be used for the open ocean and sea-ice covered domains. Furthermore, when moving from one circulation model to another, biogeochemical models will behave differently as a result of differences in the physical model (Skogen and Moll, 2005). Both these changes require adjustments to the model formulation and parameters to give good result in the focus regions. ECOSMO II(CHL) most notably introduce chlorophyll a as a prognostic variable. Allowing for a flexible chlorophyll-to-carbon ratio is more realistic and has been shown to be more stable when chlorophyll is assimilated (Ciavatta et al., 2011). This addition allows the direct assimilation of ocean color observations into the forecasting and reanalysis systems. The description of the model changes, added components and the evaluation of the ECOSMO II(CHL) results within the North Atlantic and Arctic form the main content of this paper.

The North Atlantic above 60°N, the focus in this paper, is a typical spring-bloom system (Longhurst, 1998; Rey, 2004). During winter, strong winds and cooling mix the water column several hundred meters and brings up nutrients-rich waters (Nilsen and Falck, 2006). Once the water column stratifies enough for the bloom to start, the diatoms dominate the system. When silicate is depleted, the smaller flagellates and dinoflagellates dominate the phytoplankton community (Rey, 2004). Sporadically there are also extensive coccolithophores blooms covering large areas (Baumann et al., 2000). The main species of mesozooplankton in this area, Calanus finmarchicus, overwinters at depth (Melle et al., 2004), therefore there is already some zooplankton biomass present at the time of the start of the spring. There is also a fall bloom present as seen from satellite observations. The areas closer to the Arctic, being covered by sea ice, have different dynamics. In sea ice covered regions, small blooms can occur in leads and under thin ice but the main bloom commences as the ice retracts (Dalpadado et al., 2020; Dong et al., 2020;

https://doi.org/10.5194/gmd-2021-279
Preprint. Discussion started: 11 November 2021


Geoscientific Model Development Discussions

Polyakov et al., 2020). Here, sea ice algae will make up some of the primary production (Gradinger, 2009) and other mesozooplankton, such as Calanus Glacialis, specialized to the sea ice environment (Melle and Skjoldal, 1998), are also important. Close to sea ice and in coastal regions, early stratification can occur when sea or land ice melts resulting in a seasonal halocline. Water masses in the eastern part of the basin are relatively warm, saline water characterizing the North Atlantic Current (Orvik et al., 2001), while in the western part of the basin has colder and fresher with an Arctic or mixed origin (Fröb et al., 2018 Yashayaev et al., 2007).

Our main objective with this paper is to provide the descriptions of the latest updates in ECOSMO II(CHL) and its coupling to HYCOM. We will particularly focus on the description of the prognostic chlorophyll a formulation. We aim to justify the use of the model formulation and the parameterization set as a model tool for open ocean simulations for various cases. We present the results from ECOSMO II(CHL) with the parameter set that was adopted from DS2013 (tuned for the North and Baltic Seas) as the reference simulation. However, as the North Atlantic and Artic Oceans have different physical and biogeochemical dynamics compared to the North and Baltic Seas (e.g. light availability, deep mixing), the current operational model in the Arctic and the next phase operational model which will replace the current one in mid 2021 use different parameter sets. We applied these 3 parameter sets on a model setup with a coarser grid than used for the operational simulations in order to allow for 2-decade long simulations for each case. We compare these cases and present the evaluation of the lower trophic level dynamics for the North Atlantic and the Arctic Ocean against local in situ observations, gridded climatology of nutrients and satellite data in Sect. 4. Following the evaluation we provide information on integrated quantities, such as annual primary production, inter-annual variability in phytoplankton production and seasonal succession of plankton functional types. We will finalize by commenting on the future updates and implementations of ECOSMO II(CHL).

2 The HYCOM-ECOSMO II(CHL) model

HYCOM-ECOSMO II(CHL) is a coupled physical-biological model (Fig. 1) where ocean physics are represented by the Hybrid Coordinate Ocean Model (HYCOM: Bleck, 2002) and the lower trophic marine biogeochemistry is resolved by ECOSMO II (Daewel and Schrum, 2013). The models are coupled online and the transport (advection and mixing) of biological state variables is handled as part of HYCOM's own native tracer-transport routines, thus both the physical and biological components use the same time stepping. The model is one-way coupled and biology does not affect model physics. HYCOM, as a hybrid vertical coordinate model, can optionally combine the depth-level (z-level), topography following and density-following (isopycnal) coordinates. In this study, we set vertical levels as the combination of z-level for the upper ocean and the mixed layer and isopycnal layers below. The upper 5 layers are always kept in z-levels ensuring a minimum vertical resolution which is important to resolve the light gradient in the upper ocean and thus representing the vertical variation in phytoplankton growth in a realistic manner. Isopycnal layers in the deep facilitates a good conservation of water-masses and tracer distributions.

https://doi.org/10.5194/gmd-2021-279
Preprint. Discussion started: 11 November 2021

Geoscientific Model Development Discussions

ECOSMO II(CHL) is a intermediate-complexity lower trophic level biogeochemical model which distinguishes four inorganic nutrients (nitrate, ammonium, phosphate and silicate) utilized by three types of phytoplankton (diatoms, flagellates and cyanobacteria). In this study, cyanobacteria are turned off, as they were parameterized to grow below a certain salinity threshold which was intended to represent the cyanobacteria in the Baltic Sea (Daewel and Schrum, 2013). Our area of concern is the high latitudes, specifically the area north of 60°N, thus the use of cyanobacteria falls short as a significant phytoplankton community for the region. Two types of zooplankton (micro- and meso-size classes) are parameterized based on their feeding preferences as herbivorous and omnivorous zooplankton and, as additional organic matters, dissolved (DOM) and particulate (detritus) organic matter are included in the model. The model uses the molar Redfield ratio between C:N:Si:P components (106 : 6.625 : 6.625 : 1), and discrete nutrients are tracked both in the water column and in the a single sediment layer.

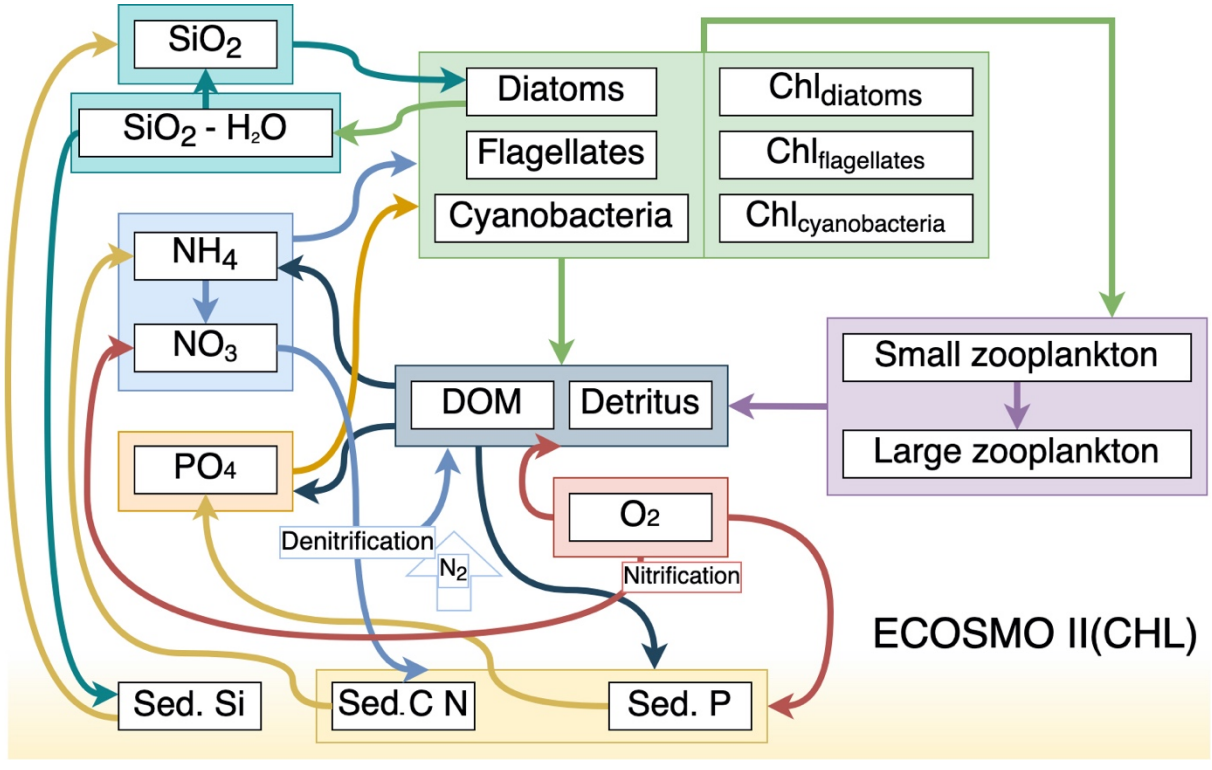

Fig. 1: Schematic diagram of biochemical interactions in ECOSMO II. (DOM: dissolved organic matter; Chl- prefixes stand for phytoplankton type specific chlorophyll a content; Sed. denote sediment pool with silicate, phosphorus and nitrate content.)

The full description of ECOSMO II is given in Daewel and Schrum (2013) (DS2013). In the following we provide a description of differences in the biogeochemical formulations in ECOSMO II(CHL) compared to DS2013. The most notable addition on DS2013 is the prognostic chlorophyll a for each phytoplankton type. The biological interaction (R_{chl_j}) term of the introduced

https://doi.org/10.5194/gmd-2021-279
Preprint. Discussion started: 11 November 2021

Geoscientific Model Development Discussions

chlorophyll a for P_1 and P_2 (diatoms and flagellates respectively) is in similar fashion to that of R_{P_j} in DS2013, as such the source terms are modified by the photoacclimation factor (ρ_{chl_j}) which accounts for the variation in chlorophyll-to-biomass ratio resulting in increased chlorophyll production under low light conditions (Geider et al., 1997), hence:

$$\boldsymbol{R_{chl_j} = \rho_{chl_j}\sigma_j\phi_{P_j}C_{P_j} - \sum_{i=1}^{2} G_i(P_j)C_{Z_i}\frac{Chl_{P_j}}{C_{P_j}} - m_{P_j}Chl_{P_j}} \quad \textbf{(1)}$$

where,

$$\boldsymbol{\rho_{chl_j} = \frac{\theta_P^{max}\phi_{P_j}C_{P_j}}{\alpha_{P_j}PAR\,Chl}} \quad \textbf{(2)}$$

$$\boldsymbol{G_i(P_j) = \sigma_{i,P_j}\frac{a_{i,P_j}C_{P_j}}{r_i+F_i}} \quad \textbf{(3)}$$

$$\boldsymbol{F_i = \sum a_{i,P_j}C_{P_j}} \quad \textbf{(4)}$$

with j = 1,2 denote the specific phytoplankton types and i = 1,2 the specific zooplankton types. C denote carbon concentration specific to P (phytoplankton) and Z (zooplankton) in mg m^{-3}, while Chl denote chlorophyll a concentration in mg m^{-3}. DS2013 give σ_j, ϕ_{P_j}, G_i and m_{P_j} as the phytoplankton maximum growth rate, growth limitation, zooplankton grazing rates and mortality rates respectively. σ_{i,P_j} denotes zooplankton specific grazing rate with a_{i,P_j} and r_i representing food preference coefficient and half saturation constant respectively. Maximum Chl-to-C ratio (θ_P^{max}) is taken from Bagniewski et al. (2011), where they have tuned those parameters for the region south of Iceland. We note that their parameterization is N-based, while ECOSMO II(CHL) uses C-based parameters, thus we applied the conversion following the C:N Redfield ratio of 6.625 resulting in flagellates and diatoms to have 0.048 and 0.037 mgChl mgC^{-1} respectively. In relation to the addition of a prognostic chlorophyll a state variable, photosynthetically active radiation I(x,y,z,t) at depth was modified to have chlorophyll a in the exponential term:

$$\boldsymbol{I(x,y,z,t) = \frac{I_s(x,y)}{2}exp\left(-k_w z - k_{Chl}\int_z^0 \sum_{j=1}^{2} Chl_{P_j}\partial z\right)} \quad \textbf{(5)}$$

where $I_s(x,y)$ is the surface net solar radiation (W m^{-2}) converted to PAR, and x, y identifies the models horizontal grid points, with z the water depth in meters. $k_w$and k_{Chl} are light extinction due to water (m^{-1}) and chlorophyll a concentration (m^2 $mgChl^{-1}$) respectively.

In addition to prognostic chlorophyll a state variables, phytoplankton and zooplankton loss terms now have an on/off switch regulated by a minimum concentration criterion preventing them from decreasing to very low concentrations. This allows them to recover and quickly respond to suitable growth conditions experienced in spring. The switch is applied to mortality and

https://doi.org/10.5194/gmd-2021-279
Preprint. Discussion started: 11 November 2021

Geoscientific Model Development Discussions

grazing terms for phytoplankton and chlorophyll a, and to mortality terms for zooplankton. The minimum concentration at which the loss terms are calculated are 0.1, 0.005 and 0.01 mgC m^{-3} for phytoplankton, chlorophyll a and zooplankton respectively.

3 Model setup and evaluation framework

Model simulations are configured on a relatively coarse grid that varies between 30 and 70 km where the highest resolutions are located in the mid-North Atlantic (Fig. 2). Although, having finer resolution was previously shown to better represent nutrient dynamics for our domain (Samuelsen et al., 2015), the main purpose of our study is to introduce the required model structure for the North Atlantic/Arctic region and the experiments, which requires numerous tests and simulations in parallel. Therefore, we concluded that having a relatively coarse grid size fits better for our purposes.

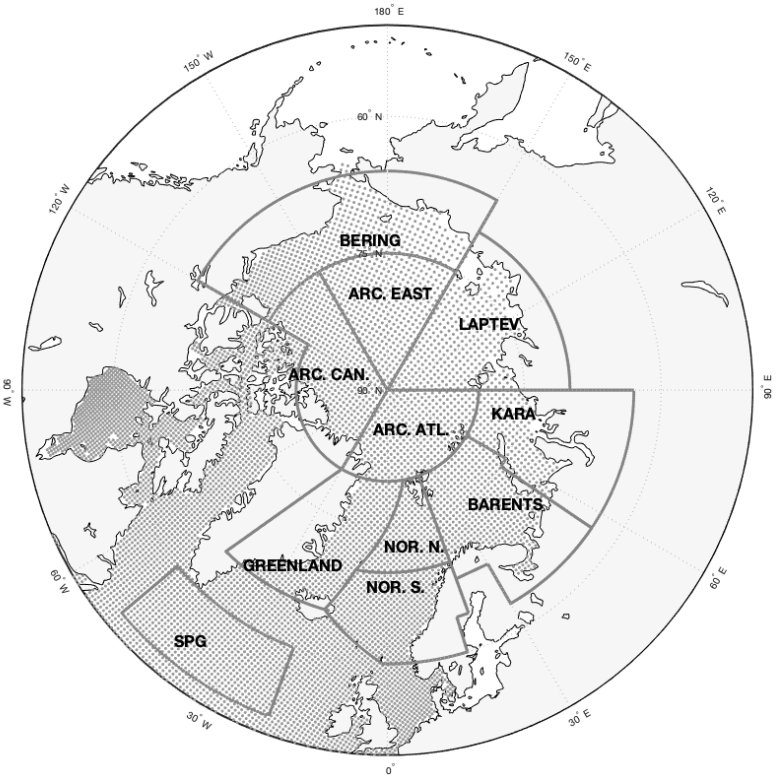

Fig. 2: Subdivision of model domain in prescribed geographical subdomains used for model quality assessments. The subdomains are as follows: Norwegian Sea South (NOR. S.), Norwegian Sea North (NOR. N.), Barents Sea (BARENTS), Kara Sea (KARA), Laptev Sea (LAPTEV), Bering Sea (BERING), Arctic-Canada (ARC. CAN.), Arctic-East (ARC. EAST), Arctic-Atlantic (ARC. ATL.), Greenland Sea (GREENLAND) and the Subpolar Gyre (SPG). The points in the oceanic regions denote the model grid coordinates. While the model domain extends down to the equatorial regions, the figure focuses on the area of interest. Note that the BERING subdomain is within the effective area of the open boundary conditions thus is relaxed to climatology.

https://doi.org/10.5194/gmd-2021-279
Preprint. Discussion started: 11 November 2021

Geoscientific Model Development Discussions

Data for atmospheric forcing is retrieved from ECMWF ERA-Interim reanalysis with 6-hour resolution (Dee et al., 2011). The variables used to force the ocean model are 10m winds, air temperature at 2 meters, dew-point temperature at 2 meters, cloud coverage and total precipitation for the physical model and surface net solar radiation for the biogeochemical model. River runoff is modelled using a hydrological model, TRIP (Oki et al., 2009), resulting in a monthly climatology dataset, so the river runoff does not include any interannual variability. River runoff affects only salinity. Nutrient loads from the rivers are derived from the modelled dataset, GlobalNEWS (Mayorga et al., 2010; Seitzinger et al., 2010), which include nitrate, phosphate and silicate. Nutrient loads were scaled by the TRIP runoff volume resulting in monthly climatology loads.

The model physics was initialized in 1989 from a spin-up simulation that started in 1948 forced by the ECHAM6 atmospheric simulation (Schubert-Frisius and Feser, 2015) . The biogeochemical model used inorganic nutrients (nitrate, phosphate and silicate) from the World Ocean Atlas 2013 (Garcia et al., 2013) monthly climatology as the initial conditions; the biomass concentrations were initialized with uniform, low values. The same climatology was used for the relaxation of temperature, salinity, nitrate, silicate, phosphate and oxygen at the open boundaries. The simulation was conducted until the end of 2010. The results are evaluated starting with the year 1991.

Table 1: Parameters that were modified between different experiments

	Model experiments		
	EXP1	EXP2	EXP3
Diatom maximum growth rate (σ_{P_1}) (1 day^{-1})	1.3	1.95	1.75
Flagellate maximum growth rate (σ_{P_2}) (1 day^{-1})	1.1	1.65	1.45
Photosynthesis efficiency ($\propto$) (m^2 W^{-1})	0.03	0.01	0.012
Mesozooplankton grazing rate on phytoplankton ($\sigma_{i,P_{j,}}$) (1 day^{-1})	0.8	1.2	1.2
Mesozooplankton grazing rate on microzooplankton ($\sigma_{i,Z_{micro,}}$) (1 day^{-1})	0.5	0.75	0.75
Microzooplankton grazing rate on phytoplankton ($\sigma_{i,P_{j,}}$) (1 day^{-1})	1.0	1.5	1.5

In this study, we employ 3 set of simulations (EXP1, EXP2 and EXP3) that use different phytoplankton growth rates, photosynthesis efficiency, and zooplankton mortality rates. EXP1 uses the DS2013 parameter set which was used for shallow and coastal seas such as the North Sea and the Baltic Sea. For the open ocean, which is the focus of this study, we introduce EXP2 (uses the parameter set for the operational forecast model for ARC MFC) and EXP3 (uses the parameter set for the next phase operational forecast model for ARC MFC currently in development). For the purpose of comparing these parameters, EXP2 and EXP3 can be considered as part of the same group against EXP1 such that in both EXP2 and EXP3, phytoplankton growth rates are set higher compared to EXP1. This reasoning behind this increase is a response to deep winter convective mixing and resulting light limitation on growth in the open ocean. Using lower growth rates (e.g. EXP1) result in a late response

https://doi.org/10.5194/gmd-2021-279
Preprint. Discussion started: 11 November 2021


Geoscientific Model Development Discussions

to light availability and recovering from high mixing in winter and delayed spring blooms. With higher growth rates, model spring bloom timing improves. However, later in summer these higher growth rates results in too much growth as the water column stabilizes. To control excessive growth of phytoplankton, zooplankton grazing rates were increased. ECOSMO II has been used as an operational model for the Arctic since 2017 and its parameterization has been tested and improved various times, more than we can document here. Thus the parameterization sets for EXP2 (current operational model) and EXP3 (next-generation operational model) are provided here as milestones for ECOSMO II development. During the continuous development of HYCOM-ECOSMO II(CHL), the parameter set for EXP3 performed better in our prior analyses and will replace the parameterization set in EXP2. To document the development process of the ECOSMO, we present all the experiments representing DS2013 (EXP1), operational model prior to 2021 (EXP2) and next-phase operational model (EXP3). The different parameters used in these simulations are given in Table 1. EXP1 is defined as the reference simulation and unless stated otherwise, results and discussions in the following sections refer to EXP1. The model evaluation is followed by an overview of the notable aspects of the simulated biogeochemistry of the North Atlantic and the Arctic Oceans.

In addition to the 3D-HYCOM-ECOSMO II(CHL) simulations, we have also performed a 1D GOTM-ECOSMO simulation at Station-M (66°N 2°E) in the Norwegian Sea to present the differences of ECOSMO II and ECOSMO II(CHL) both visually and statistically. This version of the model employs GOTM (General Ocean Turbulence Model; Burchard et al., 2006). The details of this setup is provided in Appendix A1. Station-M is a long-term time-series station and is representative of the Norwegian Sea dynamics and data from Station-M is often used for the development of ECOSMO. The dynamics shown in Appendix A1 is expected to be valid for each model point, thus can be used as a showcase for the new chlorophyll a specific addition. Apart from the improvement of model chlorophyll a results, the addition of dynamic chlorophyll a establishes a higher level of functionality of ECOSMO such that phytoplankton functional types now have their unique carbon:chlorophyll a ratios, initial slope of P-I curves which enables better adaptability to different environments, and the model now has better integration with observation systems (e.g. remote sensing) and future improvements toward bio-optical modelling.

4 Model evaluation

In this section, we present a selection of model results to provide an overview of the performance of ECOSMO II(CHL). While the model domain extends to the equatorial regions, our focus is on the Nordic Seas and the Arctic. We present the evaluation of the observable model output against in situ data with the relevant statistics. The focus of this assessment is on the key parameters of the chemical and biological fields on a regional scale where the subdomains defined for model assessment is given in Fig. 2. This approach allows for assessment of the local biogeochemical characteristics of the model. The purpose of this assessment is twofold: (1) to assess the model formulation and its parameterization as a regional hindcasting and forecasting tool, as a component of CMEMS and (2) to introduce the model's use as a tool for scientific studies.

https://doi.org/10.5194/gmd-2021-279
Preprint. Discussion started: 11 November 2021


Geoscientific Model Development Discussions

4.1 Observations

Monthly inorganic nutrient data (nitrate, silicate and phosphate) from World Ocean Atlas 2013 (WOA13; Garcia et al., 2013) were used to quantify the model's consistency with the large-scale climatological nutrient distributions. The WOA13 data were horizontally averaged in the model subdomains presented in Fig. 2. Modelled inorganic nutrients were vertically interpolated to 5 and 100 meters matching the WOA13 depth levels, spatially averaged within the subdomains and monthly averaged in time to construct corresponding regional time-series. Nitrate, silicate, phosphate and chlorophyll a in situ data from Institute of Marine Research (2018) were used for the statistical evaluation of the model results.

Very few direct observations of primary production are available in our focus region. We have therefore used reported values from the literature for evaluating the estimated magnitude of primary production (cf. Sect. 5 for the references). ESA Ocean Colour CCI v5.0 (Sathyendranath et al., 2019) daily surface chlorophyll a and downwelling attenuation coefficient at 490 nm (kd490) at 4km x 4km spatial resolution were used for evaluation. This dataset is derived from multiple sensors: SeaWIFS, MODIS Aqua, MERIS, SeaWIFS LAC and VIIR. We used this dataset for the years 1998-2010. Chlorophyll a and kd490 were remapped to the model grid and the model chlorophyll a was processed by averaging within the 1/kd490 (m) depth. In the cases that kd490 data were missing, 1/kd490 value was set to 10 meters. Processed model chlorophyll a was then statistically analyzed using the OC-CCI chlorophyll a, and from this point on, OC-CCI chlorophyll a is referred to as the satellite chlorophyll a. Satellite and model data covering the ocean topography shallower than 100 meters were masked out.

4.2 Statistical methods

We used the Institute of Marine Research (2018) dataset for inorganic nutrients and chlorophyll a to construct the statistical analyses. The statistical analyses cover 1991-2010 period and only the quality-controlled data were considered. For each in situ data point, the date and the corresponding horizontal model coordinate were identified and modeled nutrient and chlorophyll a were vertically interpolated to the depth of the in situ data point . We computed percent bias (% bias), root mean square error (rmse), correlation (corr) and normalized standard deviations (nstd) for the co-located data:

$$\%\,\boldsymbol{bias} = (\sum(\boldsymbol{M}-\boldsymbol{O})*\mathbf{100})/\sum\boldsymbol{O} \quad (6)$$

$$\boldsymbol{rmse} = \sqrt{\sum(\boldsymbol{M}-\boldsymbol{O})^2/\boldsymbol{N}} \quad (7)$$

$$\boldsymbol{corr} = (\sum(\boldsymbol{M_i}-\bar{\boldsymbol{M}})(\boldsymbol{O_i}-\bar{\boldsymbol{O}}))/\left(\sqrt{\sum(\boldsymbol{M_i}-\bar{\boldsymbol{M}})^2\sum(\boldsymbol{O_i}-\bar{\boldsymbol{O}})^2}\right) \quad (8)$$

$$\boldsymbol{nstd} = \left(\sqrt{(\sum(\boldsymbol{M_i}-\bar{\boldsymbol{M}})^2)/\boldsymbol{N}}\right)/\left(\sqrt{(\sum(\boldsymbol{O_i}-\bar{\boldsymbol{O}})^2)/\boldsymbol{N}}\right) \quad (9)$$

where M = estimated, O = observed, N = number of data points and i the individual sample. These statistics were applied to the whole simulated period but are specific to each subdomain for regional evaluations.

https://doi.org/10.5194/gmd-2021-279
Preprint. Discussion started: 11 November 2021

Geoscientific Model Development Discussions

4.3 Evaluation of the reference simulation (EXP1) against in situ data

Fig. 3 and Fig. 4 show ECOSMO II(CHL)'s performance in representing the upper 100 m concentrations of macronutrients nitrate, silicate and phosphate against monthly climatology and co-located in situ data respectively. In the case of climatological comparisons, model and observed time series are represented at the surface (5 m) and at 100 m. The model is generally in good agreement with the seasonality in climatology representing the high concentrations in winter and the drawdown of nutrients in summer, but with noticeably higher winter nutrients in the Barents Sea both at the surface and at 100 m. Note that the number of samples for the monthly climatology vary between months and regions (Fig. A2) here number of samples for winter months are significantly lower than the rest of the year. The modeled Norwegian Sea silicate concentrations are notably higher in winter at the surface and throughout the year at 100 m. Considering the consistent agreement of modeled and observed nitrate and phosphate for the Norwegian Sea and the subpolar gyre region, the simulated high silicate suggests that further tuning may be required for silicate uptake by diatoms, diatom and opal silicate sinking rates or the remineralization rates of opal. The adopted 1:1 ratio of nitrate to silicate cellular structure of phytoplankton may not be as applicable for the region. We note that although on average modeled silicate is higher than observed, occasionally diatom productivity was limited by silicate as values approached 1 mmol L^{-1} (Fig. Fig. 4c and d). The standard deviations of both the observed and modeled nutrients are large in the case of the Barents and Norwegian Seas. The monthly modeled nutrients correspond very well with the climatological values for the surface waters in the southern regions (Norwegian Sea and SPG regions) indicating satisfactory model performance on large scale productivity and its seasonal variability in these regions.

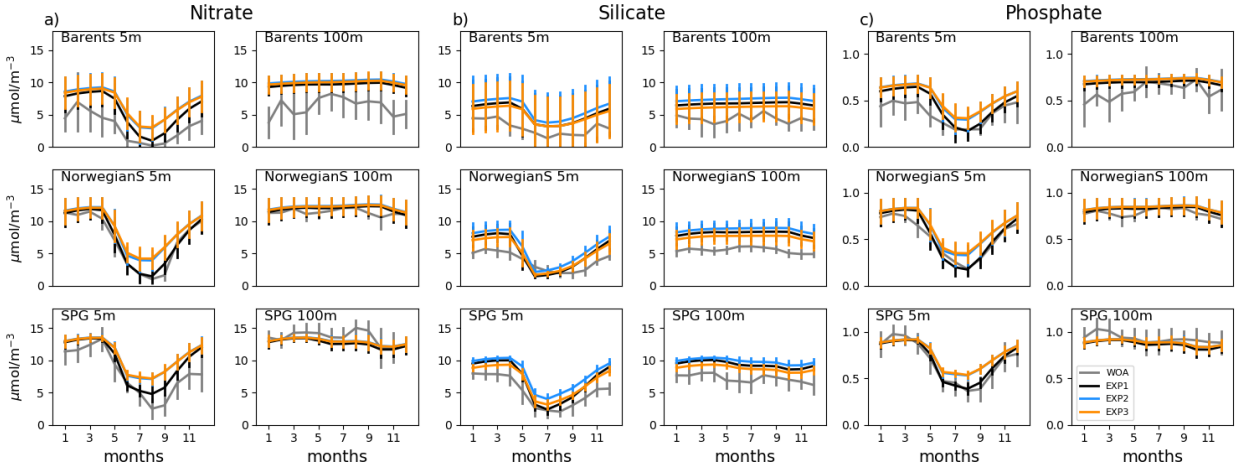

Fig. 3: Evaluation of seasonal cycle at 5 m and 100 m nutrients for the model (black lines) vs WOA18 (grey lines) regional monthly averages in the selected areas Barents, NorwegianS and SPG of the model domain for (a) nitrate, (b) silicate, and (c) phosphate. Model experiment (EXP1: solid, EXP2: dashed, EXP3: dotted) and WOA18 spatial standard deviations are plotted for each month as vertical lines). The number of observations for the WOA18 time-series is given in Figure A2.

For nitrate, model and in situ data correlations are higher than 0.83 for the three regions, with higher correlations at the higher latitudes (Table 2). One possible reason for the slight differences in correlations between lower and higher latitudes is the

https://doi.org/10.5194/gmd-2021-279
Preprint. Discussion started: 11 November 2021

Geoscientific Model Development Discussions

timing of the sampling. The majority of the sampling in the southern subdomains are held earlier in the year compared to the northern subdomains. As the model consistently initiates the spring bloom later than what is observed, a consequence of the physical model mixing scheme, it results in a later drawdown of nutrients, thus weaker correlations. The consistent late spring bloom was also noted in previous Nordic Seas modeling studies using HYCOM as the physics model (Samuelsen et al., 2009 and 2015) and they related the bloom-timing issue to the physics model or the missing phytoplankton convection process of early seeding of the spring bloom by phytoplankton that was convected in winter. However, apart from the bloom timing, correlations higher than 0.72 for silicate and 0.83 for nitrate and phosphate in general represent a good agreement on the timing and depth of nutrient variability.

Normalized standard deviations (nstd) for nitrate are within 0.6 - 0.72 indicating that the model underrepresents the amplitude of the observed variability. The model has biases between 0.65 – 0.8 mmolN m^{-3} for the Norwegian Sea, where the bias is 2 mmolN m-3 for the Barents Sea. For the case of root mean square error (rmse), modeled nitrate has errors between 2.47 – 3.34 mmolN m^{-3}. The simulated regional inorganic nutrients against in situ data are depicted in Fig. 4 where we make a point-by-point comparison of the modeled and observed inorganic nutrients. While the statistics cover every data point, Fig. 4 depicts the upper 100 m. The observed upper 100 m nitrate maximum reach 14 mmolN m^{-3} while the modeled nitrate maximum is ~11 mmolN m^{-3} in the Barents Sea (Fig. 4a), whereas the nitrate maxima are similar (Fig. 4b) for the Norwegian Sea. The source of the lower bias and rmse for the Norwegian Sea is also evident in Fig. Fig. 4b where the model to observed data points are more scattered around the 1-to-1 line compared to Fig. 4a.

Table 2: Simulation statistics (model vs in situ) specific to each region

Variable	Region	CorrCoef			Norm. StdDev			Bias (%)			RMSE (mmol m^{-3})		
		Exp1	Exp2	Exp3	Exp1	Exp2	Exp3	Exp1	Exp2	Exp3	Exp1	Exp2	Exp3
nitrate	Barents	0.88	0.86	0.86	0.79	0.63	0.60	13.5	31.3	30.5	2.43	3.34	3.34
	NorwegianN	0.89	0.87	0.87	0.84	0.66	0.64	0.7	9.0	8.6	1.94	2.39	2.39
	NorwegianS	0.83	0.80	0.80	0.83	0.73	0.72	1.9	7.8	6.7	2.25	2.51	2.47
silicate	Barents	0.78	0.74	0.78	1.16	1.18	0.98	71.8	98.8	59.5	2.62	3.41	2.23
	NorwegianN	0.72	0.67	0.74	1.07	1.02	0.94	46.8	61.7	37.9	2.89	3.49	2.46
	NorwegianS	0.73	0.67	0.74	1.02	1.00	0.91	39.9	53.0	31.0	2.63	3.19	2.26
phosphate	Barents	0.90	0.88	0.88	0.80	0.63	0.61	0.7	13.9	14.7	0.13	0.17	0.17
	NorwegianN	0.90	0.88	0.89	0.94	0.75	0.72	0.0	7.1	7.4	0.11	0.13	0.13
	NorwegianS	0.83	0.81	0.81	0.95	0.84	0.82	-1.4	3.8	3.8	0.13	0.14	0.14
chlorophyll *a*	Barents	0.38	0.29	0.3	0.97	0.61	0.57	6.2	-62.1	-61.7	0.95	0.92	0.90
	NorwegianN	0.41	0.33	0.34	2.06	1.25	1.22	68.0	-26.7	-25.1	1.49	1.03	1.00
	NorwegianS	0.23	0.19	0.20	1.50	1.06	0.97	20.3	-36.4	-39.0	1.76	1.46	1.40

For silicate, model and in situ data correlations (Table 2) range between 0.74 – 0.78, and, similar to nitrate, correlations are slightly higher at the higher latitudes. However, silicate variability due to uptake is only dependent on diatom productivity thus

https://doi.org/10.5194/gmd-2021-279
Preprint. Discussion started: 11 November 2021


Geoscientific Model Development Discussions

a direct relation to nitrate dynamics should not be expected. Both, the Barents and Norwegian Sea modeled upper 100 m maximum are higher than the observations with model biases between 1.47 – 1.82 mmolSi m^{-3} and rmse between 2.26 – 2.46 mmolSi m^{-3}. The model performs well for the silicate nstd with values very close to 1 (0.91 – 0.98) indicating the model represents the amplitude in silicate seasonal variability well. The model code limits the uptake of silicate below 1.0 mmolSi m^{-3} concentration where the effect is visible in Fig. 4c,d. The sources of high model biases and rmse's are also evident in these figures where the scattered data points are mostly below the 1-to-1 line.

The phosphate statistics are similar to those of nitrate, an expected result as all phytoplankton consume phosphate with a fixed Redfield N:P ratio. Correlations are between 0.81 – 0.89 with higher values at the higher latitudes. The nstd's (Table 2) are slightly better than those of nitrate with values between 0.61 – 0.82 indicating that the model underestimates the amplitude in phosphate variability. In agreement with the underestimated amplitude in variability, observed phosphate maximum for the upper 100m (not shown) reach 1.25 mmolP m^{-3}, where model maximum for all regions are ~1.0 mmolP m^{-3}. In terms of biases (0.026 – 0.08 mmolP m^{-3}) and RMSE's (0.13 – 0.17 mmolP m^{-3}), the model simulates phosphate better than nitrate and silicate.

https://doi.org/10.5194/gmd-2021-279
Preprint. Discussion started: 11 November 2021

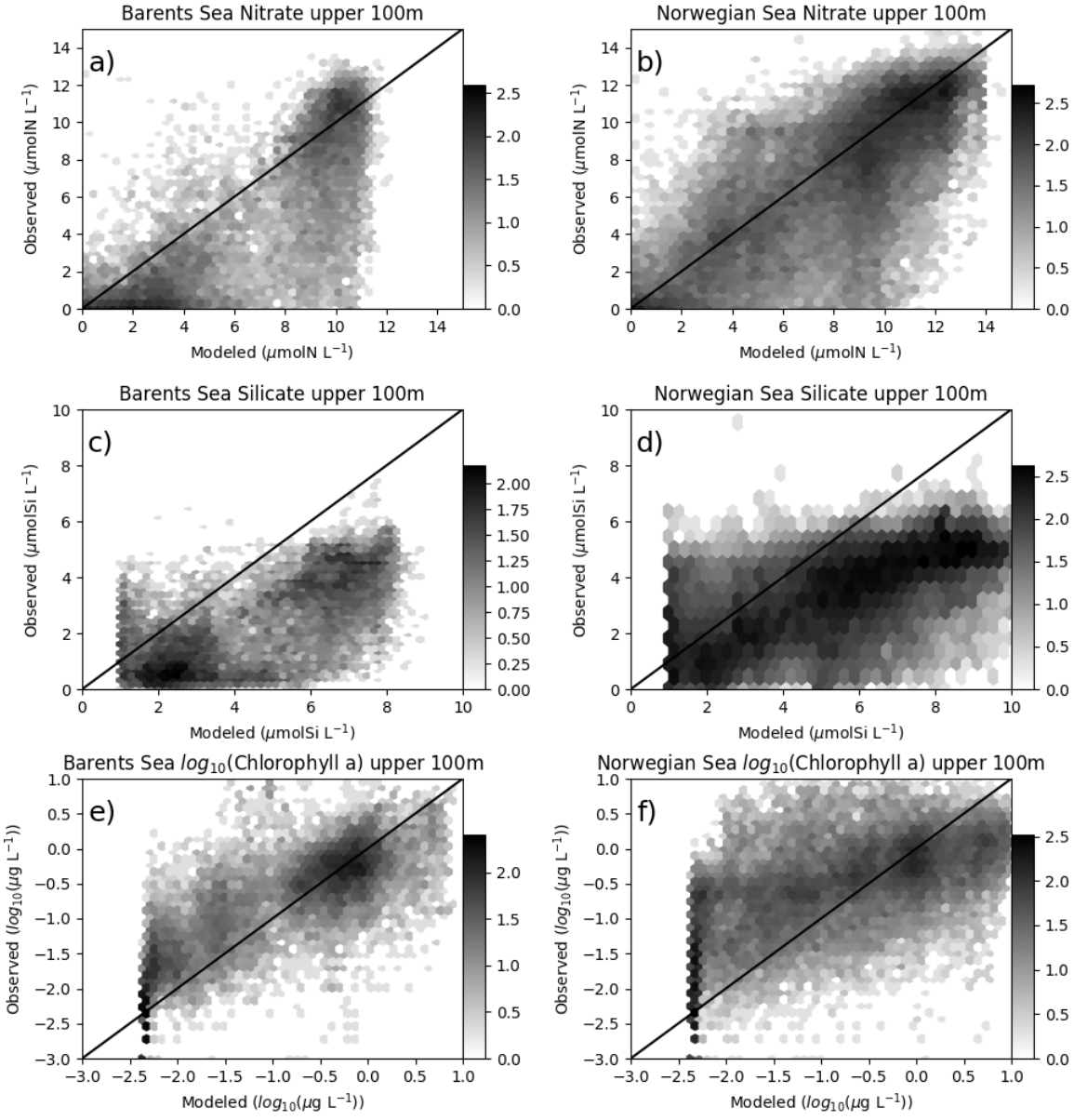

Fig. 4: Co-located modeled (EXP1) and in situ upper 100m nitrate (a) Barents Sea, (b) Norwegian Sea, silicate (c) Barents Sea, (d) Norwegian Sea and chlorophyll (e) Barents Sea, (f) Norwegian Sea comparisons. Log10 number of points are represented in hexagonal local clusters with shades of grey. Only the upper 100 m points are plotted.

310 In situ chlorophyll a correlations for the upper 100 m (Table 2) are between 0.23 – 0.41, which are below those of inorganic nutrients. However, the model performs well in terms of nstd's especially for the Norwegian Sea (0.97 and 1.2) and acceptable (0.57) for the Barents Sea. The model has minor negative biases (0.12 – 0.27 mg m^{-3}) and rmse's between 0.95 – 1.76 mg m^{-3}. The concentration range (Fig. 4f) are similar (0 – 10 mg m^{-3}) for both the observed and modeled for the Norwegian Sea indicated by nstd's near 1.0, but the points are scattered away from the 1-to-1 line indicating the low correlations. Model

https://doi.org/10.5194/gmd-2021-279
Preprint. Discussion started: 11 November 2021


Geoscientific Model Development Discussions

chlorophyll a maximum is limited to 8 mg m-3 for the Barents Sea (Fig. 4e) where the observations show values above 10 mg m^{-3} indicating the lower nstd's underestimating the amplitude of variability.

5 Simulated biogeochemistry of the North Atlantic and the Arctic

Primary production (PP) is the foundation for all marine biological production and the most frequently observed rate in BGC models. Still, there are only few observations of primary production available in the ocean as a whole, but the high Arctic is particularly poorly sampled (Matrai et al., 2013). Because the model does not have an explicit term for respiration, we can only extract gross primary production from the model, which is then compared to observations. The modelled gross annual primary production ranges from above 200 gC m^{-2} y^{-1} in the southern part of the model domain to almost zero in the central Arctic and features a gradual decrease from 144.26 gC m^{-2} y^{-1} to 41.48 gC m^{-2} y^{-1} from lower latitudes (SPG) towards the higher latitudes (Barents) respectively, with a sharp decrease to very low values (<6 gC m^{-2} y^{-1}) in the sea ice covered areas (Fig. 5, Table 3) as a consequence of light limitation. Rey (1981) estimated the primary production in the Norwegian Coastal Current to range from 90 - 120 gC m^{-2} y-1, which agrees well with the values from this model (Fig. 5), although the used coarse resolution model does not represent a very distinct coastal current. Previous studies have estimated the primary production in the Fram Strait from 50 - 80 gC m^{-2} y^{-1} (Hop et al., 2006), while our model show values of 90-100 gC m^{-2} y^{-1} in the Atlantic waters and up to 30-60 gC m^{-2} y^{-1} on its western side. Lee et al. (2015) compared multiple Arctic models against in situ observations. Only a few of these observations were in the central Arctic while the majority were located in the Chukchi Sea, which is very close to the zone where the model is relaxed to climatology. They found a median value of all Arctic observations of 246 mgC m^{-2} d^{-1} which corresponds to about 90 gC m^{-2} y^{-1}. The regional estimates of primary production were similar, but the shelf regions were the most productive. The model results for the regions surrounding the central Arctic ocean fall in the range of this estimate, but observation base estimates for the central Arctic, although only few are available, are higher than the model results. From Lee et al. (2015) the primary production estimates from the central Arctic varied between 10 and 100 mgC m^{-2} d^{-1} (~4 - 40 gC m^{-2} y^{-1}) while the model is below 1 gC m^{-2} y^{-1}. In the model formulation, the ice is blocking more light than what is realistic and ice leads cannot be resolved, so our estimate is expected to be low in ice covered regions. It is known that both melt ponds and leads can act as windows into the ocean, facilitating blooms (Assmy et al., 2017). The light below the ice will be improved in future versions of the model system. In situ observations in the Arctic range up to more than 5000 mgC m^{-2} d^{-1}, the model does not reproduce the extremes in primary production, but the mean values are overall consistent with available observations.

For the Norwegian and Barents Seas, the modeled primary production show distinct seasonal patterns with almost negligible productivity between November – April due to low light availability (Fig. 6). During the onset of the spring bloom, production is notably at its highest during May – June followed by a gradual decrease towards late fall. Regional differences in primary production are also evident in year-round time-series, where the Norwegian Sea primary productivity is significantly higher

https://doi.org/10.5194/gmd-2021-279
Preprint. Discussion started: 11 November 2021

Geoscientific Model Development Discussions

than the Barents Sea productivity. Southern part of the Norwegian Sea (NorwegianS) has a notably earlier (~2 weeks) bloom compared to the northern counterpart.

Table 3: Regional vertically integrated (0–200 m) annual primary production (gC m^{-2} y^{-1}) and simulation averaged vertically integrated (0–200 m) plankton functional type biomass (gC m^{-2}) in EXP1. See Sect. 3 for the definition of the regions. Note that the BERING subdomain is within the effective area of the open boundary conditions thus is relaxed to climatology.

Region	PP gC m^{-2} y^{-1}	DIA gC m^{-2}	FLA gC m^{-2}	MIC gC m^{-2}	MES gC m^{-2}
Barents	41.48	0.311	0.243	0.061	0.847
NorwegianN	98.2	1.191	0.442	0.12	1.673
NorwegianS	89.26	0.82	0.441	0.108	1.551
ArcAtl	2.6	0.051	0.027	0.007	0.044
Laptev	2.31	0.063	0.013	0.004	0.031
ArcEast	0.22	0.024	0.019	0.002	0.009
ArcCan	0.17	0.019	0.016	0.002	0.002
Bering	6.3	0.117	0.021	0.01	0.091
Kara	5.28	0.094	0.026	0.009	0.067
Greenland	34.95	0.399	0.153	0.046	0.595
SPG	144.26	1.56	0.647	0.214	2.128

The simulated seasonal evolution of primary production reflects the growth of plankton functional types, with diatoms (compared to flagellates) being the dominant type in the Nordic Seas spring bloom (Fig. 7). A relatively minor flagellate bloom follows a few weeks after that of diatoms. Zooplankton biomass increase from May – June in response to phytoplankton growth and is maintained till the end of the year. Note that ECOSMO II(CHL) allows zooplankton to feed on detritus, which contribute to zooplankton sustaining growth beyond the seasons of phytoplankton activity. Towards the lower latitudes, south of 45 ºN, flagellates maintain a similar annually integrated productivity (~1.5 vs ~1.0 (gC m^{-2})) to that of diatoms (Fig. 5c-e). Mesozooplankton are the dominant grazer in all regions (Fig. 5d-f). Similar to primary production, the NorwegianN and NorwegianS functional type biomasses are higher compared to Barents functional type biomasses with daily 200m averaged biomasses reaching 75 – 100 mgC m^{-3} for diatoms and mesozooplankton in the Norwegian Sea, and ~50 mgC m^{-3} for the Barents Sea respectively. For both Barents and Norwegian Sea, flagellate and microzooplankton biomasses do not exceed ~25 mgC m^{-3} during their highest productive seasons (Fig. 7).

https://doi.org/10.5194/gmd-2021-279
Preprint. Discussion started: 11 November 2021

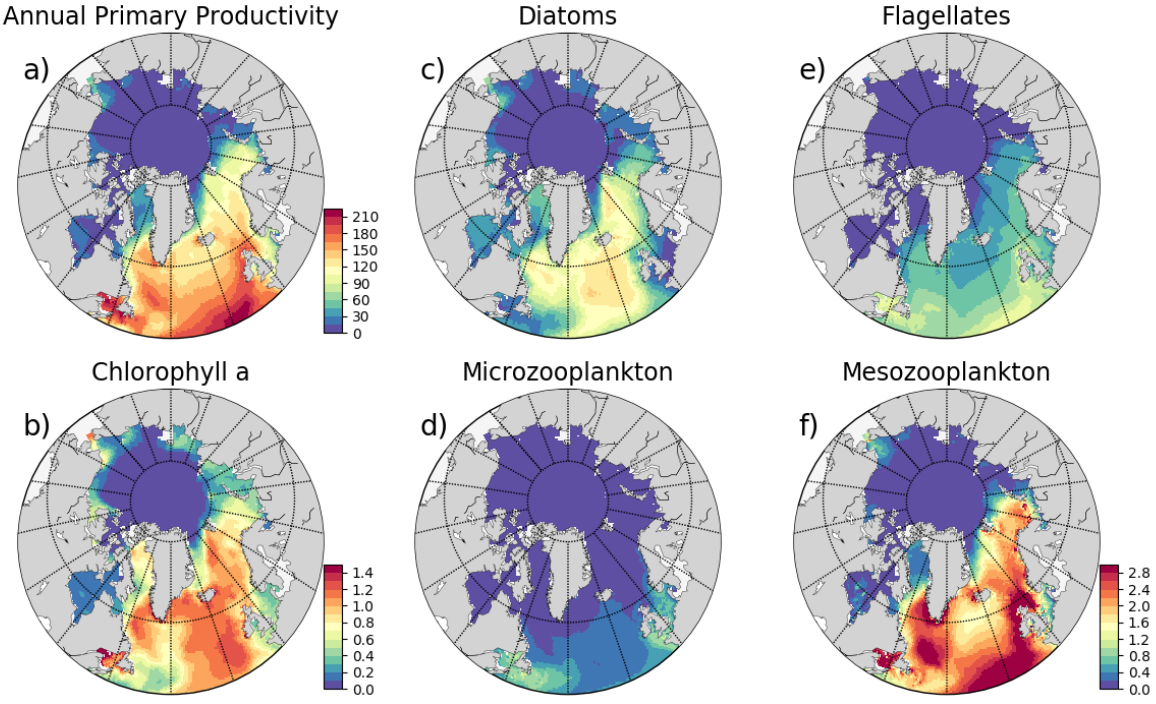

Fig. 5: Simulation averaged (EXP1) model results; (a) vertically integrated (0–200 m) annual primary production (gC m^{-2} y^{-1}), (b) annually averaged surface chlorophyll a (mg m^{-3}), and simulation averaged vertically integrated (0–200 m) plankton functional type biomass (gC m^{-2}) (c) diatoms, (d) microzooplankton, (e) flagellates, (f) mesozooplankton. The colorbar to Figure f applies to Figures c, d, e and f.

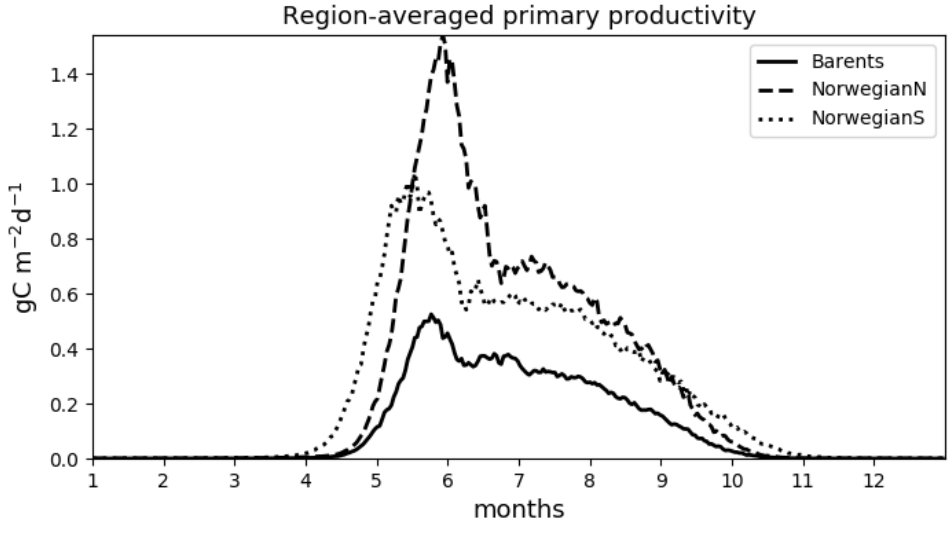

Fig. 6: Simulated (EXP1) time-series of 0-200 m integrated primary productivity (gC m^{-2} d^{-1}) for different regions: (a) Barents, (b) NorwegianN and (c) NorwegianS. See Table 3 for annually averaged primary productivities.

https://doi.org/10.5194/gmd-2021-279
Preprint. Discussion started: 11 November 2021

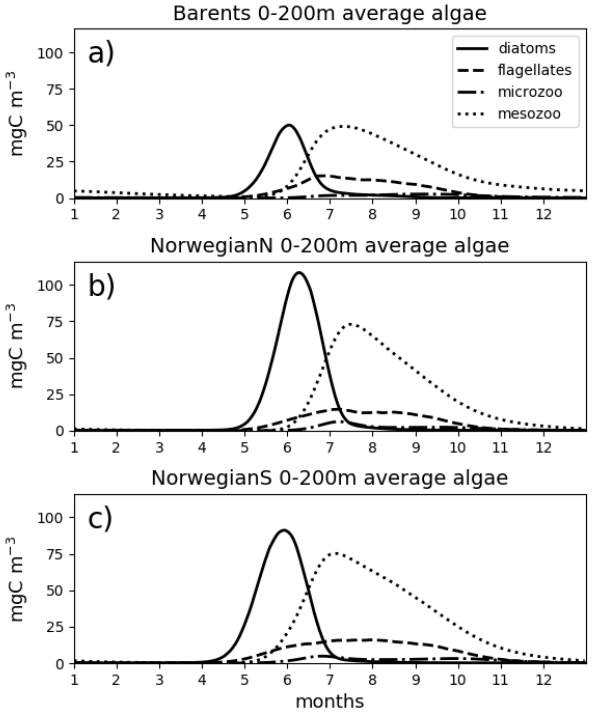

375 **Fig. 7: Simulated (EXP1) daily averaged time-series of each plankton functional type (average of 0-200 m depth range).**

The model predicts regionally high annually averaged inorganic nutrient concentrations for the subpolar gyre compared to the Norwegian and Barents Seas which is also reflected in monthly and regionally averaged concentrations (Fig. 8) with relatively lower concentrations in the coastal regions of the Nordic Seas compared to their offshore regions. The model also predicts a 380 contrast between nutrient specific regions of high concentrations. Nitrate concentrations are higher at the lower latitudes, whereas phosphate and silicate are higher towards the higher latitudes. These features generally agree with the features of WOA2018 data (Fig. 8). The high overall nutrient concentrations near the Bering Sea and high silicate concentrations at the Siberian coast due to river discharge is more pronounced in the climatology data. As mentioned earlier, the model does not allow light to penetrate sea-ice. For this reason, the model overestimates surface inorganic nutrients compared to climatology 385 below the sea-ice as these nutrients are not consumed by primary production, but are only affected by transport and remineralization. Overall, the model performs well in terms of N/P molar ratios (NO3/PO4; Fig. A3). Both model and climatology suggest a higher N/P ratio for the Nordic Seas and lower latitudes (~12-16). At the Barents Sea coast, the climatology has a lower N/P ratio (<7) but has a high ratio at the ice-edge region (>17). In contrast, the model predicts a more regular N/P distribution with a gradual decrease from 16 to 12 from lower to higher latitudes at the Barents Sea.

390

https://doi.org/10.5194/gmd-2021-279
Preprint. Discussion started: 11 November 2021

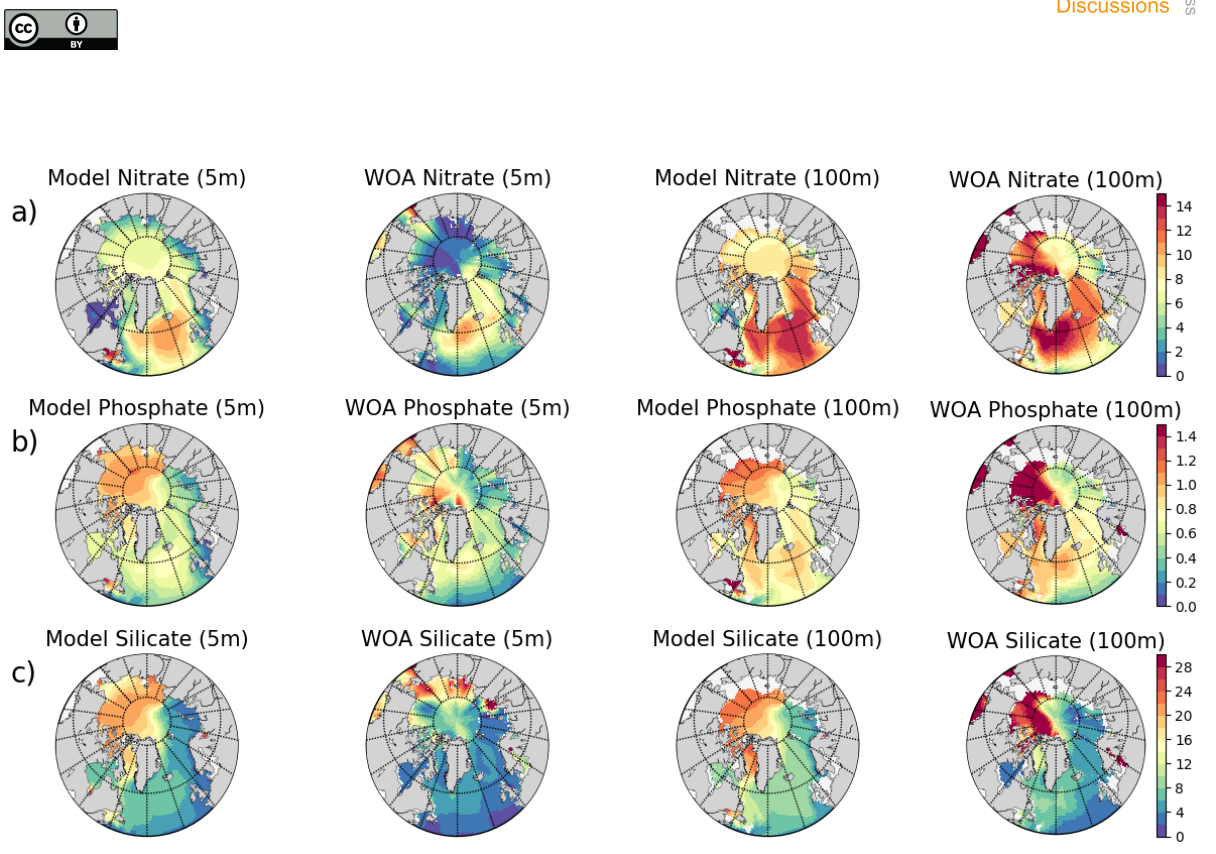

Fig. 8: Simulation averaged (EXP1; mmol m^{-3}) (a) nitrate, (b) phosphate and (c) silicate for 5 and 100 meters isodepth and corresponding WOA2018 annual climatologies.

6 Model experiments

395

Here we present the evaluation of each model experiment against satellite chlorophyll a. While this evaluation is a supplement to the evaluation performed in Sect. 4 against in situ data for the reference simulation (EXP1), the evaluation for EXP2 and EXP3 are provided here for the assessment of the model parameterization described in Sect. 3, and how they perform in relation to EXP1. Since the parameters in EXP2 and EXP3 are used in open-ocean operational models, their performance in
400 representing satellite chlorophyll a is vital for the assimilation of chlorophyll a in the operational model. The comparison of co-located surface in situ, model and satellite data are given in Figure 9 and their statistics are summarized in Table 4. The purpose of comparing the satellite data to both in situ and the model is to evaluate the satellite product itself for the region, as satellite products are prone to uncertainties based on the used algorithms and is related to differences in absorption and backscattering properties of phytoplankton and concentrations of colored-dissolved organic matter (CDOM) and minerals
405 (Dierssen, 2010). Thus, in the absence of in situ data, we have a better understanding when model and satellite data are compared. Table 5 summarizes model statistics against satellite data, which is both independent of the in situ samples and, due to the volume of satellite data, the statistics here are based on a much more extensive dataset compared to the statistics in Table 4.

https://doi.org/10.5194/gmd-2021-279
Preprint. Discussion started: 11 November 2021

Geoscientific Model Development Discussions

For the three regions of interest, the satellite data have a negative bias against the in situ data (Table 4). The %bias is minor for the Barents region (-5.32%), but for the Norwegian Sea, the biases are -21.34% and -16.11% for the north and south respectively. The nstd's range between 0.51 – 0.65 mg m^{-3} suggesting that satellite chlorophyll a underrepresents the amplitude of the in situ observed variability of chlorophyll a. Satellite chlorophyll a rmse's range between 0.6 – 0.8 mg m^{-3}.

Table 4: Estimated chlorophyll a statistics against in situ surface chlorophyll a. Data points that are co-located with in situ data locations only are used. Co-located satellite data is also compared against in situ data for reference. See Sect. 3 for the calculation of statistics.

	Barents			NorwegianN			NorwegianS		
	Bias (%)	**RMSE** (mg m^{-3})	**Norm. StdDev**	**Bias (%)**	**RMSE** (mg m^{-3})	**Norm. StdDev**	**Bias (%)**	**RMSE** (mg m^{-3})	**Norm. StdDev**
Satellite	-5.32	0.60	0.65	-21.34	0.66	0.51	-16.11	0.80	0.53
EXP1	39.75	1.21	1.52	178.25	2.85	3.50	140.56	2.74	2.54
EXP2	-55.69	1.08	1.15	50.76	1.87	2.68	39.59	1.89	1.85
EXP3	-51.21	1.03	1.02	43.32	1.67	2.43	23.50	1.66	1.59

Table 5: Model chlorophyll a statistics against satellite data. See Sect. 3 for the calculation of statistics.

	Barents				NorwegianN				NorwegianS				SPG			
	Bias (%)	**RMSE** (mg m^{-3})	**Norm. StdDev**	**Corr Coef**	**Bias (%)**	**RMSE** (mg m^{-3})	**Norm. StdDev**	**Corr Coef**	**Bias (%)**	**RMSE** (mg m^{-3})	**Norm. StdDev**	**Corr Coef**	**Bias (%)**	**RMSE** (mg m^{-3})	**Norm. StdDev**	**Corr Coef**
EXP1	56.23	2.21	1.45	0.0	203.51	2.95	4.52	0.0	130.72	2.45	4.03	0.0	140.33	2.28	5.60	0.01
EXP2	-15.73	1.78	1.05	0.05	59.69	1.88	3.16	0.28	26.84	1.69	2.97	0.25	10.34	1.29	3.33	0.27
EXP3	-22.83	1.67	0.91	0.05	52.12	1.75	2.95	0.28	17.70	1.51	2.67	0.26	8.12	1.25	3.23	0.26

EXP1 has higher chlorophyll a concentration compared to EXP2 and EXP3. This is visually evident when model and satellite data are plotted against in situ data (Fig. 9) where EXP2 and EXP3 generally form clusters distinct from EXP1. EXP1 chlorophyll a are mainly located at the right side of the 1-to-1 line suggesting a positive bias against the in situ data evident in Table 4 with 39.75% for the Barents Sea and 178.25% and 140.56% for north and south Norwegian Sea respectively. The rmse's and nstd's are also higher compared to EXP2 and EXP3. Relatively, EXP1 is the least representative of the in situ data among the experiments. EXP2 and EXP3 overestimate chlorophyll a for the Norwegian Sea with %biases ranging between 23.5% - 50.76%, and overrepresenting the amplitude of variability with nstd's ranging between 1.59 – 2.68 mg m^{-3}. For the Barents Sea, while EXP2 and EXP3 have negative biases and rmse's around ~1 mg m^{-3}, their nstd's show that they correctly estimating the amplitude of variability. With a much larger number of data points, the model error statistics computed from satellite data are similar (Table 5) with EXP1 resulting in the highest chlorophyll a values statistically performing the worst compared to EXP2 and EXP3. Notably, EXP2 and EXP3 biases are much better compared to the statistics against in situ with the exception of NorwegianN, with less errors overall. We note that the in situ data are restricted in both, the overall amount amount as well as the season, as most of the data are from late spring and onwards whereas satellite data also cover earlier

https://doi.org/10.5194/gmd-2021-279
Preprint. Discussion started: 11 November 2021

Geoscientific Model Development Discussions

parts of the year under favourable weather conditions. Satellite data also increase the regional coverage of the statistical analyses where SPG region statistics show that EXP2 and EXP3 outperform the EXP1 statistics (Table 5).

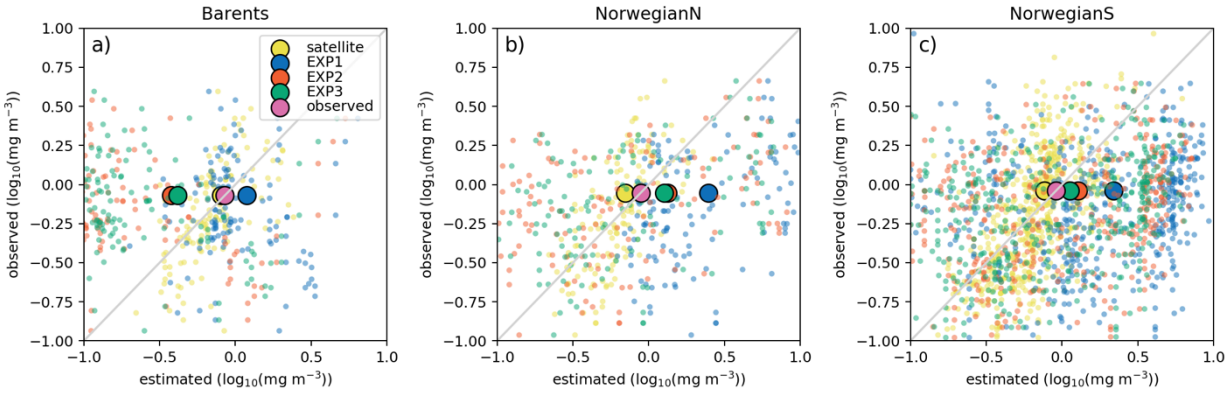

Fig. 9: Estimated surface chlorophyll a data against in situ observations (log10(mg m^{-3})). Region-wide averages are depicted with the large markers representative of the individual points depicted with the same colors in the background with smaller-sized markers.

The consistent higher bias of EXP1 compared EXP2 and EXP3 can be explained by its higher photosynthesis efficiency (Table 1). EXP1 perform a very fast phytoplankton response to light availability during the spring bloom period where light availability is increased resulting in a steep curve where chlorophyll a concentrations are notably higher compared to the observations (results not shown) evident in the high %biases, whereas EXP2 and EXP3 have closer concentrations during spring bloom. Originally, ECOSMO II parameterization was set for the North Sea and the Baltic Sea with different light conditions. In the open ocean such a high response curve overestimate the bloom. However, winter convective mixing is very deep in the Nordic Seas, thus the light is a limiting factor on growth. To overcome deep mixing and prevent a late spring bloom, the phytoplankton were allowed to have very high growth rates for EXP2 and relatively less higher growth parameters were set for EXP3. Statistically and visually (Fig. 9), both EXP2 and EXP3 are very similar, with EXP3 performing statistically slightly better. Experiment statistics for inorganic nutrients are very similar in all experiments (Table 2). Taking into account the model performance overall, EXP1 parameterization perform better for the coastal regional seas as it was originally designed for (DS2013), but for the case of open ocean, EXP3 parameterization has the better performance.

7 Conclusions

In this paper we provided the mathematical description of an updated version of ECOSMO II which is used as the biogeochemical model for the operational forecasting of the Arctic Ocean, its evaluation against in situ and remote sensing data, and analyses on different parameterizations targeting chlorophyll a dynamics.

https://doi.org/10.5194/gmd-2021-279
Preprint. Discussion started: 11 November 2021


Geoscientific Model Development Discussions

The qualitative and quantitative evaluation of the model results of inorganic nutrients, chlorophyll a and primary production has demonstrated that the model is consistent with the large-scale climatological nutrient settings, and is capable of representing regional and seasonal changes. The model primary production agrees with previous measurements. Our parameterization experiments showed that for the open ocean domains, model chlorophyll a benefits from using higher phytoplankton growth and zooplankton grazing rates with less photosynthesis efficiency compared to the original implementation of ECOSMO II for the North Sea and the Baltic Sea which represent coastal domains. We related the improved effect on chlorophyll a to better timing of the spring bloom in the North Atlantic and Nordic Seas due to higher growth rates.

With improved chlorophyll a implementation, i.e. the use of phytoplankton-specific dynamic chlorophyll a-to-carbon ratios in reference to a fixed ratio in the original model, ECOSMO II(CHL) with its intermediate complexity definition of the North Atlantic and Arctic Ocean ecosystem structure including a sediment layer is a capable modeling tool for both scientific and operational use. The modeling structure presented in this study, including the physical model, HYCOM, forms the basis of the modeling framework that the future updates will build on and ECOSMO II(CHL) is thus currently being developed to include migratory fish and a dynamic particle sinking scheme that will broaden the scope of the model.

Appendices

A.1 Comparison of ECOSMO II and ECOSMO II(CHL) chlorophyll a dynamics at Station-M

In this section we present a 1D model setup at Station-M (66ºN 2ºE) in the Norwegian Sea using GOTM as the physics model using 1-hour interval atmospheric forcing. The location of the station resides in the Norwegian Sea South region depicted in Figure 2. We performed a 27-year run starting in 1990 using realistic constant values for the biogeochemical variables and considered the first 5 years as the spin-up period. Model results and statistics provided in Figure A1 and Table A1 are calculated from the last 22 years. Statistical analysis was performed using the Station-M time-series data which is included in the Institute of Marine Research (2018) dataset described in 4.2. We assumed a carbon:chlorophyll a ratio of 60 for ECOSMO II to perform the analyses using the total phytoplankton biomass. The chlorophyll a depiction from ECOSMO II therefore indicate only the phytoplankton biomass and does not affect the model in any way, whereas in the case of ECOSMO II(CHL), chlorophyll a is explicitly represented for each phytoplankton type and the results are real model chlorophyll a outputs. EXP3 parameters are used for these simulations.

The major difference between the 2 variants of ECOSMO II is that in the case of CHL variant, the model carbon:chlorophyll a ratio adapts to the light availability, where abundant light results in a higher ratio (days 140 – 250; Fig. A1d) at the surface,

https://doi.org/10.5194/gmd-2021-279
Preprint. Discussion started: 11 November 2021

Geoscientific Model Development Discussions

lower ratio in case of lower light availability either due to seasons or high attenuation due to high chlorophyll a at the surface. The latter case can be observed around day 150 (Fig. A1d).

A significant difference in the results is that the non-CHL variant simulates higher chlorophyll a concentrations (Fig A1a-c) assuming a 60 carbon:chlorophyll a ratio which is a representative average ratio for most of the productive period for ECOSMO II(CHL) (Fig. A1d). The difference is more pronounced in the upper 10 meters due to higher carbon:chlorophyll a ratio (~100) under abundant light. While both simulations are statistically similar in general, especially the deeper euphotic zone (40 – 80 m), ECOSMO II(CHL) statistically performs better at 0 - 20 m range (Table A1).

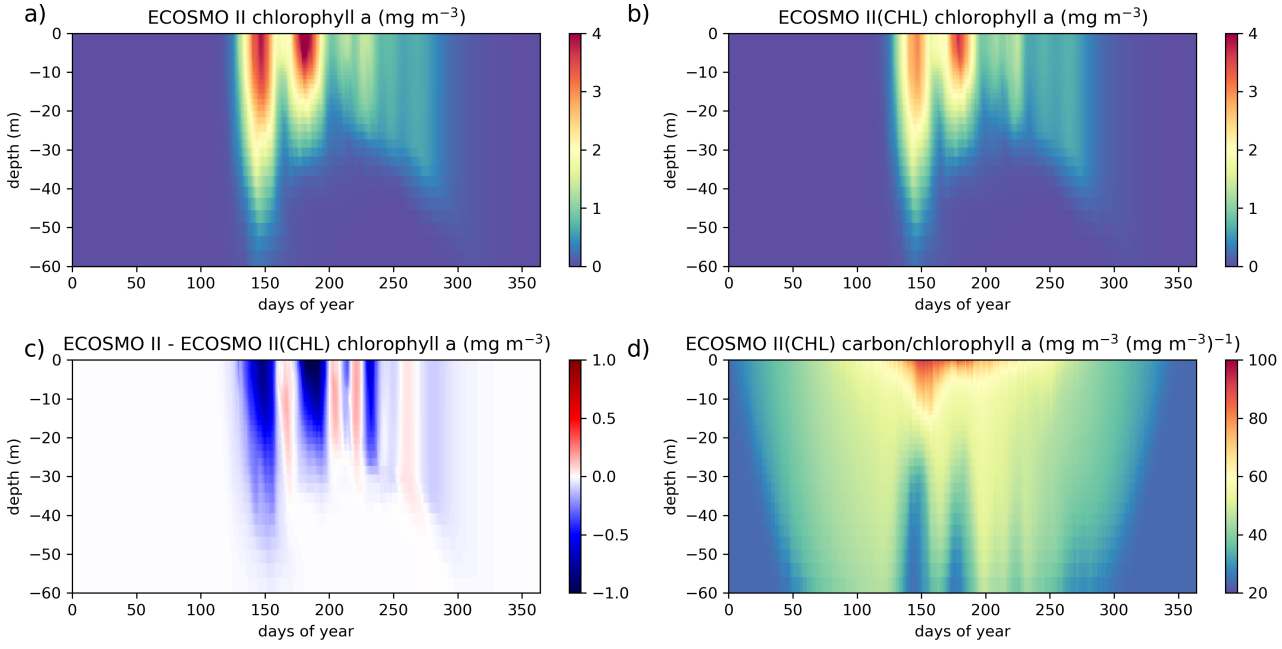

Fig. A1: ECOSMO II chlorophyll a dynamics is compared to ECOSMO II(CHL) using a 27-year (1990 – 2016) 1D simulation at Station-M (66ºN 2ºE) in the Norwegian Sea. Results provided here are the averages of the last 22 years (1995 – 2016) of the simulations given as annual climatologies. Figures a and b depict chlorophyll a concentrations of ECOSMO II and ECOSMO II(CHL) respectively, c depicts the chlorophyll a difference of the 2 simulations, and d depict the diatom and flagellate averages of carbon:chlorophyll a ratios.

Table A1 : Comparison of ECOSMO II and ECOSMO II(CHL) chlorophyll a statistics against in situ data depicting 20 m sections of the upper 80 m water column using an output from a 1D model simulated at Station-M (66ºN 2ºE) in the Norwegian Sea.

	ECOSMO II				ECOSMO II(CHL)			
	Bias (%)	RMSE (mg m^{-3})	Norm. StdDev	CorrCoef	Bias (%)	RMSE (mg m^{-3})	Norm. StdDev	CorrCoef
0 – 20 m	42.76	1.27	2.14	0.38	21.97	1.05	1.78	0.39
20 – 40 m	-23.96	0.68	1.25	0.40	-33.37	0.62	1.06	0.42

https://doi.org/10.5194/gmd-2021-279
Preprint. Discussion started: 11 November 2021

Geoscientific Model Development Discussions

40 – 60 m	-62.99	0.49	0.72	0.26	-68.35	0.48	0.61	0.28
60 – 80 m	-89.75	0.18	0.15	0.44	-91.73	0.19	0.12	0.45

A.2 World Ocean Atlas 2018 supplementary figures

In this section we provide the supplementary figures for Section 4.3 and 5 by presenting the number of observations used for the statistical analyses in WOA2018 dataset for each region and inorganic nutrient (Fig. A2) and annual averages of NO_3/PO_4 molar ratios (Fig. A3).

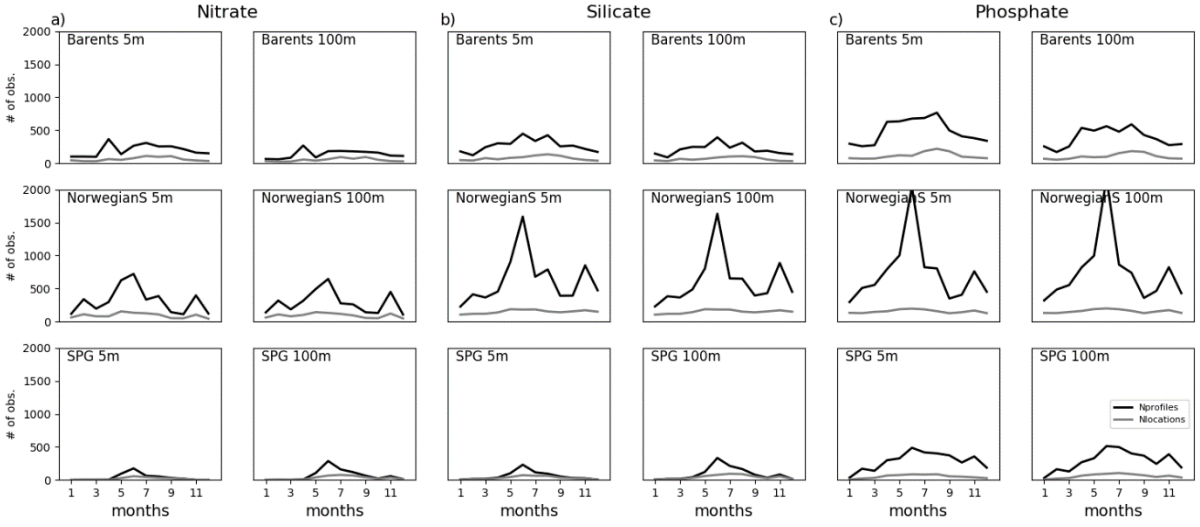

Fig. A2: Number of observations for the WOA18 inorganic nutrient time-series given in Figure 4. Multiple profiles exist for some of the locations, thus the black lines denote the total number of profiles and grey lines denote the number of different locations for those profiles.

https://doi.org/10.5194/gmd-2021-279
Preprint. Discussion started: 11 November 2021

Geoscientific Model Development Discussions

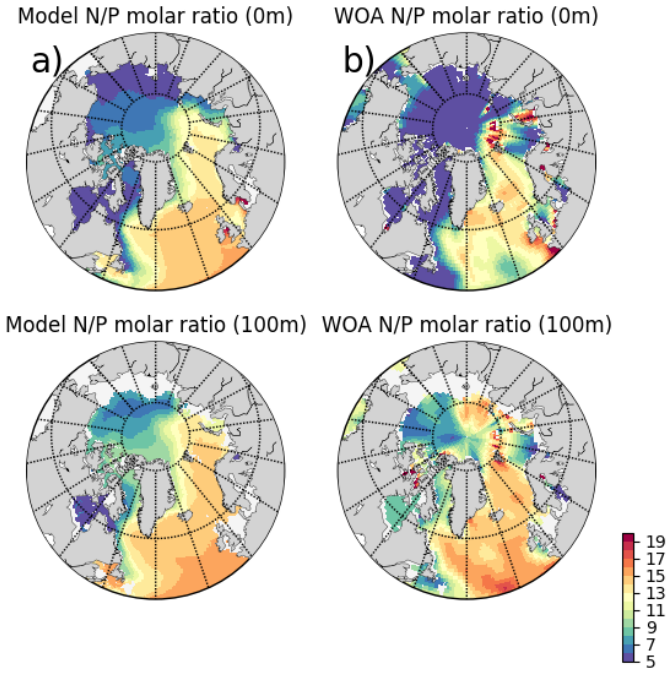

Fig. A3: Simulated and WOA2018 inorganic nutrients annual averages NO_3/PO_4 molar ratios, a) model, b) WOA2018 for 5 and 100 meters isodepth.

Code availability

The exact version of the model used to produce the results used in this paper is archived on Zenodo (https://doi.org/10.5281/zenodo.5606973; Lisæter et al. (2021)) including the input data and scripts to run the model and produce plots for all the simulations presented in this paper. They are openly available under Creative Commons Attribution 4.0 International license. HYCOM version used is 2.2.37 and the ECOSMO II(CHL) code is available in HYCOM_2.2.37/CodeOnly/src_2.2.37/nersc/ECOSMO where m_ECOSM_biochm.F is the master biogeochemical code. The model setup used here is located under "model_setup/expt_09.0/SCRATCH/" directory. After the compilation following the procedure documented in "Doc" folder, the executable copied to the SCRATCH folder should be able to replicate the model presented here. Further instructions are provided in the README file. The different parameters given for each experiment in the manuscript can be applied to "HYCOM_2.2.37/CodeOnly/src_2.2.37/nersc/ECOSMO/ECOSMparam1.h". The model is set to produce daily averaged binary files, but scripts to convert the binary files to netcdf files are included in "MSCPROGS/src". The model code is written in FORTRAN. Model results provided in the manuscript are located under "model_output" directory.

https://doi.org/10.5194/gmd-2021-279
Preprint. Discussion started: 11 November 2021


Geoscientific Model Development Discussions

Author contribution

VCY and AS designed the experiments and VCY carried them out. UD is the developer of ECOSMO II and together with AS, they coupled ECOSMO II to HYCOM physics model. VCY has built the ECOSMO II(CHL) version on ECOSMO II. The physics model setup for this study was mainly prepared by AS, and the preparation of the biogeochemical setup, sensitivity analyses and model evaluation were carried out by VCY. VCY prepared the manuscript with contributions from all co-authors.

Competing interests

The authors declare that they have no conflict of interest.

Acknowledgements

VCY and AS acknowledge the support of CMEMS for the Arctic MFC. UD was supported through ZOOMBI (CMEMS 66-SE-CALL2). The computations were performed on the Norwegian Sigma2 infrastructure under the projects NN9481K and NS9481K. Visualization of model results and revision of this manuscript is also supported by the European Space Agency through the Cryosphere Virtual Laboratory (CVL, grant no. 4000128808/19/I-NS)

References

Assmy, P. et al. (2017) 'Leads in Arctic pack ice enable early phytoplankton blooms below snow-covered sea ice', Scientific Reports. Nature Publishing Group, 7(1), pp. 1–9. doi: 10.1038/srep40850.

Bagniewski, W. et al. (2011) 'Optimizing models of the North Atlantic spring bloom using physical, chemical and bio-optical observations from a Lagrangian float', Biogeosciences, 8(5), pp. 1291–1307. doi: 10.5194/bg-8-1291-2011.

Baumann, K. H., Andruleit, H. A. and Samtleben, C.: Coccolithophores in the Nordic Seas: comparison of living communities with surface sediment assemblages, Deep. Res. Part Ii-Topical Stud. Oceanogr., 47(9–11), 1743–1772, 2000.

Bleck, R. (2002) 'An oceanic general circulation model framed in hybrid isopycnic-Cartesian coordinates', Ocean Modelling. Elsevier, 4(1), pp. 55–88. doi: 10.1016/S1463-5003(01)00012-9.

Burchard, H., Bolding, K., Kühn, K., Meister, A., Neumann, T., andUmlauf, L.: Description of a flexible and extendable physical-biogeochemical model system for the water column, J. MarineSyst., 61, 180–211, 2006.

https://doi.org/10.5194/gmd-2021-279
Preprint. Discussion started: 11 November 2021

Ciavatta, S. et al. (2011) 'Can ocean color assimilation improve biogeochemical hindcasts in shelf seas?', Journal of Geophysical Research. Blackwell Publishing Ltd, 116(C12), p. C12043. doi: 10.1029/2011JC007219.

Daewel, U. and Schrum, C. (2013) 'Simulating long-term dynamics of the coupled North Sea and Baltic Sea ecosystem with ECOSMO II: Model description and validation', Journal of Marine Systems. Elsevier B.V., 119–120, pp. 30–49. doi: 10.1016/j.jmarsys.2013.03.008.

Dalpadado, P., Arrigo, K. R., van Dijken, G. L., Skjoldal, H. R., Bagøien, E., Dolgov, A. V., Prokopchuk, I. P. and Sperfeld, E.: Climate effects on temporal and spatial dynamics of phytoplankton and zooplankton in the Barents Sea, Prog. Oceanogr., 185(April), 102320, doi:10.1016/j.pocean.2020.102320, 2020.

Dee, D. P. et al. (2011) 'The ERA-Interim reanalysis: Configuration and performance of the data assimilation system', Quarterly Journal of the Royal Meteorological Society, 137(656), pp. 553–597. doi: 10.1002/qj.828.

Dierssen, H. M.: Perspectives on empirical approaches for ocean color remote sensing of chlorophyll in a changing climate, Proc. Natl. Acad. Sci. U. S. A., 107(40), 17073–17078, doi:10.1073/pnas.0913800107, 2010

Dong, K., Kvile, K. Ø., Stenseth, N. C. and Stige, L. C.: Associations among temperature, sea ice and phytoplankton bloom dynamics in the Barents Sea, Mar. Ecol. Prog. Ser., 635, 25–36, doi:10.3354/meps13218, 2020.

Fröb, F., Olsen, A., Pérez, F. F., Garciá-Ibáñez, M. I., Jeansson, E., Omar, A. and Lauvset, S. K.: Inorganic carbon and water masses in the Irminger Sea since 1991, Biogeosciences, 15(1), 51–72, doi:10.5194/bg-15-51-2018, 2018.

Garcia, H. E. et al. (2013) 'NOAA Atlas NESDIS 76 WORLD OCEAN ATLAS 2013 Volume 4: Dissolved Inorganic Nutrients (phosphate, nitrate, silicate)', 4(September).

Geider, R. J., MacIntyre, H. L. and Kana, T. M. (1997) 'Dynamic model of phytoplankton growth and acclimation: Responses of the balanced growth rate and the chlorophyll a:carbon ratio to light, nutrient-limitation and temperature', Marine Ecology Progress Series, 148(1–3), pp. 187–200. doi: 10.3354/meps148187.

Gradinger, R.: Sea-ice algae: Major contributors to primary production and algal biomass in the Chukchi and Beaufort Seas during May/June 2002, Deep. Res. Part II Top. Stud. Oceanogr., 56(17), 1201–1212, doi:10.1016/j.dsr2.2008.10.016, 2009.

https://doi.org/10.5194/gmd-2021-279
Preprint. Discussion started: 11 November 2021

Hop, H. et al. (2006) 'Physical and biological characteristics of the pelagic system across Fram Strait to Kongsfjorden', Progress in Oceanography. Pergamon, 71(2–4), pp. 182–231. doi: 10.1016/j.pocean.2006.09.007.

595 Institute of Marine Research (2018). Næringssalt-, oksygen- og klorofylldata i norske havområder fra 1980-2017.

Lee, Y. J. et al. (2015) 'An assessment of phytoplankton primary productivity in the Arctic Ocean from satellite ocean color/in situ chlorophyll- a based models', Journal of Geophysical Research: Oceans. Blackwell Publishing Ltd, 120(9), pp. 6508–6541. doi: 10.1002/2015JC011018.

600

Lisæter, K. A., Counillon, F., Xie, J., Hansen, C., Samuelsen, A., Yumruktepe, V. Ç., Daewel, U., Schrum, C., Evensen, G., and Bertino, L. (2021). HYCOM-ECOSMOII(CHL) a marine biogeochemical model for the North Atlantic and the Arctic model code and configuration. Zenodo. https://doi.org/10.5281/zenodo.5606973

605 Longhurst, A. R.: Ecological biogeography of the sea, Academic Press, San Diego, USA., 1998.

Matrai, P. A., Olson, E., Suttles, S., Hill, V., Codispoti, L. A., Light, B., & Steele, M. (2013). Synthesis of primary production in the Arctic Ocean: I. Surface waters, 1954–2007. Progress in Oceanography, 110, 93-106. doi: 10.1016/j.pocean.2012.11.004.

610

Mayorga, E. et al. (2010) 'Global Nutrient Export from WaterSheds 2 (NEWS 2): Model development and implementation', Environmental Modelling and Software. Elsevier, 25(7), pp. 837–853. doi: 10.1016/j.envsoft.2010.01.007.

Melle, W. and Skjoldal, H. R.: Reproduction and development of Calanus finmarchicus, C-glacialis and C-hyperboreus in the
615 Barents Sea, Mar. Ecol. Ser., 169, 211–228, 1998.

Nilsen, J. E. Ø. O. and Falck, E.: Variations of mixed layer properties in the Norwegian Sea for the period 1948-1999, Prog. Oceanogr., 70(1), 58–90, doi:10.1016/j.pocean.2006.03.014, 2006.

620 Oki, T. et al. (2009) 'Design of Total Runoff Integrating Pathways (TRIP)—A Global River Channel Network', http://dx.doi.org/10.1175/1087-3562(1998)002<0001:DOTRIP>2.3.CO;2. doi: 10.1175/1087-3562(1998)002<0001:DOTRIP>2.3.CO;2.

Orvik, K., Skagseth, Ø. and Mork, M.: Atlantic infow to the Nordic Seas : current structure and volume fluxes from moored current meters , VM-ADCP and SeaSoar-CTD observations , 1995 1999, Deep Sea Res. Part I Oceanogr. …, 48, 937–957,
625 2001.

Polyakov, I. V., Alkire, M. B., Bluhm, B. A., Brown, K. A., Carmack, E. C., Chierici, M., Danielson, S. L., Ellingsen, I., Ershova, E. A., Gårdfeldt, K., Ingvaldsen, R. B., Pnyushkov, A. V., Slagstad, D. and Wassmann, P.: Borealization of the Arctic Ocean in Response to Anomalous Advection From Sub-Arctic Seas, Front. Mar. Sci., 7(July), doi:10.3389/fmars.2020.00491, 2020.

Rey, F.: Phytoplankton: the grass of the sea, in The Norwegian Sea Ecosystem, edited by H. R. Skjoldal, Tapir Academic Press, Trondheim., 2004.

Samuelsen, A., Hansen, C. and Wehde, H. (2015) 'Tuning and assessment of the HYCOM-NORWECOM V2.1 biogeochemical modeling system for the North Atlantic and Arctic oceans', Geoscientific Model Development, 8(7), pp. 2187–2202. doi: 10.5194/gmd-8-2187-2015.

Samuelsen A, Huse G, Hansen C (2009) Shelf recruitment of Calanus finmarchicus off the west coast of Norway: role of physical processes and timing of diapause termination. Mar Ecol Prog Ser 386:163-180. https://doi.org/10.3354/meps08060

Sathyendranath, S. et al. (2019) 'An ocean-colour time series for use in climate studies: The experience of the ocean-colour climate change initiative (OC-CCI)', Sensors (Switzerland). MDPI AG, 19(19). doi: 10.3390/s19194285.

Schrum, C., Alekseeva, I. and John, M. S. (2006) 'Development of a coupled physical-biological ecosystem model ECOSMO. Part I: Model description and validation for the North Sea', Journal of Marine Systems, 61(1–2), pp. 79–99. doi: 10.1016/j.jmarsys.2006.01.005.

Schubert-Frisius, M. and Feser, F. (2015) 'Global High Resolution Climate Reconstruction with ECHAM6 using the spectral nudging technique, run by Helmholtz-Zentrum Geesthacht', https://cera-www.dkrz.de/WDCC/ui/cerasearch/entry?acronym=CLISAP_MPI-ESM-XR_t255l95. World Data Center for Climate (WDCC) at DKRZ. doi: 10.1594/WDCC/CLISAP_MPI-ESM-XR_T255L95.

von Schuckmann, K. et al. (2016) 'The Copernicus Marine Environment Monitoring Service Ocean State Report', Journal of Operational Oceanography. Taylor & Francis, 9, pp. s235–s320. doi: 10.1080/1755876X.2016.1273446.

Seitzinger, S. P. et al. (2010) 'Global river nutrient export: A scenario analysis of past and future trends', Global Biogeochemical Cycles. John Wiley & Sons, Ltd, 24(4), p. n/a-n/a. doi: 10.1029/2009GB003587.

Skogen, M. D. and Moll, A. (2005) 'Importance of ocean circulation in ecological modeling: An example from the North Sea', Journal of Marine Systems. Elsevier, 57(3–4), pp. 289–300. doi: 10.1016/j.jmarsys.2005.06.002.

https://doi.org/10.5194/gmd-2021-279
Preprint. Discussion started: 11 November 2021

Yashayaev, I., Bersch, M. and van Aken, H. M.: Spreading of the Labrador Sea Water to the Irminger and Iceland basins, Geophys. Res. Lett., 34(10), 1–8, doi:10.1029/2006GL028999, 2007.